# Architecturally-Induced Tricontinuous Cubic Morphology in Compositionally Symmetric Miktoarm Starblock Copolymers

**Yiannis Tselikas and Nikos Hadjichristidis***

*Department of Chemistry, University of Athens, Athens, Panepistimiopolis, Greece*

**Robert L. Lescanec**

*Department of Polymer Science, The University of Southern Mississippi, Hattiesburg, Mississippi 39406*

**Christian C. Honeker, Meinhard Wohlgemuth, and Edwin L. Thomas***

*Department of Materials Science, Massachusetts Institute of Technology, Cambridge, Massachusetts 02139*

*Received October 10, 1995; Revised Manuscript Received February 13, 1996*[⊗]

ABSTRACT: We report the synthesis and morphological characterization of a *miktoarm* block copolymer architecture: $(PS_{\alpha M}-PI_M)_n-(PS_M-PI_{\alpha M})_n$, where $M \sim 20\,000$, $n = 1, 2$, and the arm asymmetry parameter $\alpha = 1$, 2, or 4 ($\alpha$ is the ratio of the outer block molecular weight to that of the inner block). These block copolymers are symmetric in overall composition and exhibit *n*- and $\alpha$-dependent microdomain morphologies. Alternating lamellae are observed for linear tetrablocks ($n = 1$), $\alpha = 1, 2, 4$, and for inverse starblock ($n = 2$), $\alpha = 1, 2$. An architecturally-induced morphological transition from lamellae to a tricontinuous cubic structure is observed with $n = 2$ and $\alpha = 4$. The formation of the tricontinuous cubic microdomain structure in this compositionally *symmetric* system is thought to relieve the overcrowding of the four peripheral PS−PI junctions by providing a curved intermaterial dividing surface with a triply periodic microdomain structure, allowing some bridging by the interior blocks of the miktoarm star.

## Introduction

The microdomain morphology of a particular copolymer is determined by the minimization of the free energy of the system. The block copolymer system adopts a periodic microdomain structure that best satisfies the constraints of interfacial energy minimization, conformational entropy maximization, and uniform segment density. It has been established[1−5] that the microstructure is a function of the volume fraction, temperature, the chemical nature of the polymeric species, and the molecular weight. The influence of copolymer architecture on the structure of the microphase separated state is much less well studied. Early work on triblock copolymers found these to behave essentially as diblocks of the corresponding composition. Investigation of star diblock copolymers found, in addition to the three classical microdomain geometries of lamellae, cylinders, and spheres, a new tricontinuous cubic structure.[6−12] The theoretical phase diagram has been studied for triblocks[13] and for star copolymers,[14] but no new phases have been predicted.

Well-defined copolymer materials of various architectures have been only recently synthesized.[15−18] The influence of chain architecture on the classic diblock morphology diagram via synthesis of a miktoarm star of the type $A_2B$ found a dramatic shift in the phase boundaries compared to classical diblocks but no new phase types.[19] Since their discovery in star diblocks, tricontinuous cubic structures have been observed in diblock, starblock, ABC triblock, and diblock−homopolymer blends at volume fractions of about 27−35% minority component.[20−25] These structures are made of two interpenetrating but nonintersecting networks of the minority block in a matrix of the other block. The polymer microphases in the networks and in the matrix are all three dimensionally continuous. In the ordered bicontinuous double diamond (OBDD) (henceforth called double diamond, DD) the interface between the two components can approximately be represented by an intermaterial dividing surface (IMDS) which exhibits constant mean curvature ($H$ = constant) at any point.[26] The IMDS is a member of the triply periodic Schwarz D minimal surface ($H = 0$) family, with $Pn\bar{3}m$ space group symmetry. The other more recently discovered cubic copolymer structure, originally referred to as the "gyroid" and henceforth called the double gyroid (DG), is associated with the Schoen G minimal surface family, with $Ia\bar{3}d$ space group symmetry.[27,28] Structures with $Pn\bar{3}m$ and $Ia\bar{3}d$ symmetry have been identified in the past in surfactant and liquid crystal systems as well.[29−31]

In the morphology diagram of any intermediate to strongly segregated diblock copolymer studied so far, the lamellar morphology dominates in a large region centered about the 50/50 volume fraction. In order to induce a new microdomain morphology at 50/50 composition, we designed architecturally complex multiblock copolymer molecules that contain several blocks of different molecular weight, while remaining symmetric in overall composition as well as being intermediate to strongly segregated. The polymeric species chosen for this purpose have the inverse starblock and linear tetrablock architecture shown in Figure 1. The copolymers were prepared by anionic polymerization and chlorosilane coupling chemistry, a synthetic approach that has been proven to produce molecules with the highest control over the composition, molecular weight distribution, and architecture. The inverse starblocks, a macromolecular architecture prepared for the first time, are made of 4 diblock arms of polystyrene and polyisoprene. Two diblocks are connected to the star center with their PS ends, while the remaining two diblocks are connected to the star center with their PI ends. The term miktoarm stars (mixed arm stars) is

[⊗] Abstract published in *Advance ACS Abstracts,* April 1, 1996.

S0024-9297(95)01508-7 CCC: $12.00 

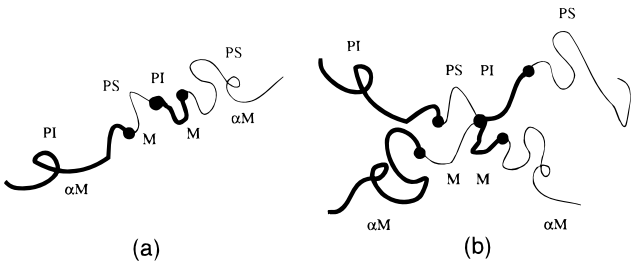


**Figure 1.** Schematic representation of the miktoarm starblock and linear tetrablock molecules. The asymmetry parameter has values $\alpha = 1$, 2, and 4. The inner block molecular weight is approximately 20 000 for all copolymers.

used to describe the stars with this architecture. The linear tetrablocks (equivalent to two-armed stars) can be seen as just one-half of the starblock molecules. In all our copolymers, the inner blocks are equal or smaller in molecular weight to the outer blocks. This is described by the arm asymmetry parameter $\alpha$ which is the ratio between the outer ($M_o$) to the inner block molecular weights ($M_i$) ($\alpha = M_o/M_i$). In all cases the overall composition is kept constant at approximately 50% by volume of each component. The structures of this series of polymers were characterized by TEM and SAXS to investigate how changes in architecture and arm asymmetry influence microdomain morphology.

## Experimental Section

The miktoarm inverse starblock and linear tetrablock copolymers were prepared by anionic polymerization using high vacuum techniques in evacuated, *n*-BuLi washed, and benzene-rinsed glass reactors. Additions of the reagents were made through fragile glass membranes (break seals) and removals of aliquots for characterization by heat sealing of constrictions. Details on the reagent purification to the standards required for anionic polymerization, and linking reactions, are described elsewhere.[15,16] *s*-BuLi, prepared in vacuo from *sec*-butyl chloride and a lithium dispersion, was the initiator and benzene the solvent for all polymerizations. Dimethyldichloro- and tetrachlorosilane were used as linking agents. Fractionation was carried out by adding methanol to a solution (~1% w/v) of the linking reaction product in toluene at room temperature. It was repeated until no precursor or undesirable byproducts were shown to be present by SEC. For the size exclusion chromatography (SEC) a Waters 501 solvent delivery pump was used, equipped with a Waters 401 differential refractometer, a Waters 486 UV detector, and four Phenomenex linear Styragel columns with porosites ranging from 500 to $10^6$ Å. The carrier solvent was THF at 30 °C pumped at a flow rate of 1 mL/min. The weight-average molecular weight was determined by low-angle laser light scattering (LALLS) in THF at 25 °C using a Chromatix KMX-6 apparatus operated at a wavelength of 6328 Å. The refractive index increment with concentration ($dn/dc$) was measured with a Chromatix KMX-16 instrument operated at the same wavelength and calibrated with NaCl standards. The number-average molecular weight was determined in toluene at 34 °C with a Wescan 230 membrane osmometer (MO). $^1$H NMR determination of the composition and microstructure of the materials was carried out in $CDCl_3$ at 30 °C using a Varian Unity Plus 300/54 instrument. For the polyisoprene blocks, the typical microstructure characteristic of anionic polymerization of isoprene in benzene was observed (10 wt % 3,4, 70 wt % cis-1,4, and 20 wt % trans-1,4). The SEC, LALLS, MO, and NMR measurements were performed following procedures published elsewhere.[15,16] The glass transition temperature of the polystyrene component was measured on a Seiko 220C DSC. Polymer degradation was checked by dissolving the annealed samples in THF and re-running SEC. All the TB samples and SB-1 showed no detectable difference. Samples SB-2 and SB-4 exhibited some slight cross-linking effects most likely due to the influence of the presence of previously unreacted linking agent.

Calculated values of the experimental quench parameter, $\chi N$ (for $T = 120$ °C), place all systems in the intermediate to strong segregation regime, based on a mean-field calculation[32] of $\chi N$ at the spinodal (see Table 3). All copolymer samples are therefore far from their estimated order−disorder transition temperature and deep into the normal lamellar morphology portion of a diblock copolymer during the 120 °C, 7-day annealing treatment.

For SAXS and TEM characterization approximately 0.4 mm thick films of the materials were quiescently cast from a dilute solution (~5% w/v) with a nearly nonselective solvent (toluene) over a period of 1 week at ambient conditions. In addition, the polymer films were dried under vacuum for 3 days at room temperature. The films were subsequently annealed above the glass transition temperatures of PS and PI components at 120 °C for 7 days under vacuum. For TEM investigation, approximately 50 nm thick sections of the block copolymers were cryomicrotomed at approximately −110 °C using a Reichert-Jung FC 4E cryoultramicrotome equipped with a diamond knife. To enhance mass−thickness contrast, the thin polymer sections were exposed to $OsO_4$ vapors for 1 h and then carbon coated to increase their stability in the electron beam. The stained sections were examined in a JEOL 200CX electron microscope operated at 200 kV in the bright field mode.

The X-ray diffraction (SAXS) data were acquired at room temperature on the Time-Resolved Diffraction Facility (station X12B) at the National Synchrotron Light Source at Brookhaven National Laboratory (BNL) using a custom-built two-dimensional gas delay-line detector (10 × 10 cm, 512 × 512 pixels), interfaced to a real-time histogramming memory system.[33] The optical system provides a doubly-focused (spot size, 0.5 × 0.5 mm fwhm) monochromatic X-ray beam (bandpass, ~$5 \times 10^{-4}$ $\Delta\lambda/\lambda$) spanning 0.9−1.5 Å (here $\lambda = 1.38$ Å was chosen). All frames were azimuthally integrated about the beam center in bins of 1 pixel width. The $q$ conversion was determined by dividing the width of each pixel (105 $\mu$m) by the sample-to-detector distance (1.86 m).

## Results and Discussion

The synthetic procedure described here is based on the same protocol Iatrou and Hadjichristidis followed for the preparation of miktoarm copolymers.[16] The basic reaction scheme is the following:

*Arm Synthesis*

$$\text{isoprene} + \text{sBuLi} \xrightarrow{\text{benzene}} \text{PI}^-\text{Li}^+ \xrightarrow[\text{THF (trace)}]{\text{styrene}} \text{PI}-\text{PS}^-\text{Li}^+ \quad \textbf{(I)}$$

$$\text{styrene} + \text{sBuLi} \xrightarrow{\text{benzene}} \text{PS}^-\text{Li}^+ \xrightarrow{\text{isoprene}} \text{PS}-\text{PI}^-\text{Li}^+ \quad \textbf{(II)}$$

*Inverse Starblock Synthesis*

$$2\mathbf{I} + \text{SiCl}_4 \xrightarrow[\text{SEC monitoring}]{\text{titration}} (\text{PI}-\text{PS})_2\text{SiCl}_2 + 2\text{LiCl} \quad \textbf{(III)}$$

$$(\text{PI}-\text{PS})_2\text{SiCl}_2 + \text{excess } \mathbf{II} \rightarrow (\text{PI}-\text{PS})_2\text{Si}(\text{PI}-\text{PS})_2 + 2\text{LiCl} \quad \textbf{(IV)}$$

*Linear Tetrablock Synthesis*

$$\mathbf{I} + \text{excess Si}(\text{CH}_3)_2\text{Cl}_2 \rightarrow (\text{PI}-\text{PS})\text{Si}(\text{CH}_3)_2\text{Cl} + \text{LiCl} \quad \textbf{(V)}$$

$$(\text{PI}-\text{PS})\text{Si}(\text{CH}_3)_2\text{Cl} + \text{excess } \mathbf{II} \rightarrow (\text{PI}-\text{PS})\text{Si}(\text{CH}_3)_2(\text{PI}-\text{PS}) + \text{LiCl} \quad \textbf{(VI)}$$

In the case of the diblock arms (**I**), after the synthesis of the polyisoprene block, a small amount of THF was

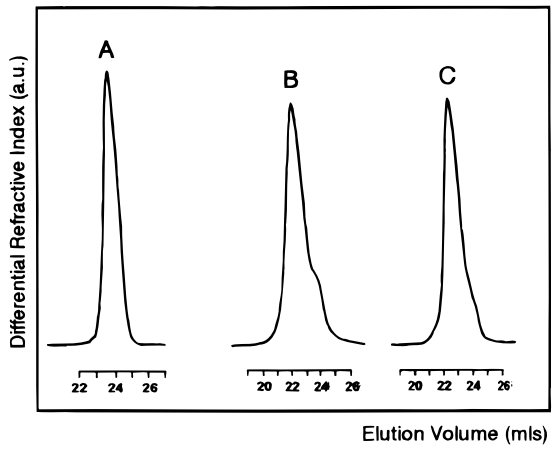


**Figure 2.** SEC chromatograms from the titration process during the synthesis of the starblock SB-1. (A) corresponds to the PI−PS$^-$Li$^+$ precursor. The (B) trace shows an intermediate step of the first two arm addition, the main peak being (PI−PS)$_2$SiCl$_2$. The (C) trace shows the end point which is determined by the trimer formation.

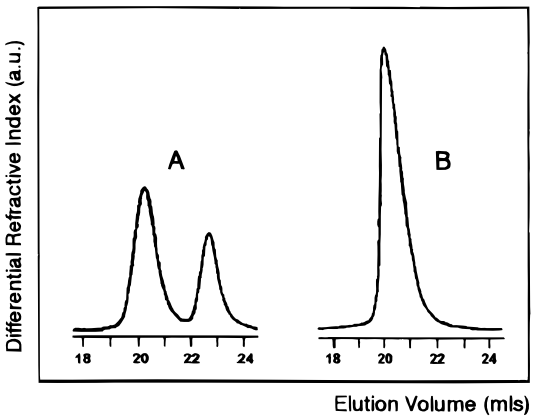


**Figure 3.** SEC of the unfractionated (A) and the fractionated (B) starblock SB-4.

added in order to promote the kinetics of initiation of the polystyrene block and thus maintain the narrow molecular weight distribution of the diblock precursor. These diblock arms were selected to react first with the chlorosilane linking agents; because of the increased steric hindrance of the polystyrene living ends, the incorporation of only two arms is better controlled.

To synthesize the inverse starblock copolymers, a dilute solution of PI−PS$^-$Li$^+$ in benzene was added dropwise to a stoichiometric amount of tetrachlorosilane ($SiCl_4$) in benzene until two chlorine atoms of the linking agent were substituted by the diblock arms. During the addition, small aliquots of the reaction solution were removed from the reactor and analyzed by SEC in order to monitor the progress of the reaction. The end point of this titration process was determined when a small shoulder at 21 mL (<1% of the dimer peak area), which corresponds to the formation of trimer, appeared in the SEC trace, as shown in Figure 2. The formation of trimer (PI−PS)$_3$SiCl is highly indicative of the completion of the titration reaction due to the large difference in the reactivity between the second and third chlorine atom toward substitution from a PS anion.[34] In all the syntheses performed in this study, a small amount of the living diblock arm was terminated, most likely due to trace impurities present in the $SiCl_4$ solution. The presence of the terminated diblock precursor was observed as a low molecular weight peak at the end point of the SEC chromatograms. The difunctional macromolecular linking agent (PI−PS)$_2$SiCl$_2$ was reacted with an excess of the PS−PI$^-$Li$^+$ living diblock arm until the remaining two chlorine atoms were quantitatively substituted, completing the synthesis of the (PI−PS)$_2$−(PI−PS)$_2$ inverse starblock copolymer. To relieve steric hindrance and facilitate the addition of the two remaining PS−PI$^-$Li$^+$ arms, their living ends were capped with 3−4 units of butadiene before the reaction with the macromolecular linking agent. The inverse starblock was then purified by fractionation. Typical SEC chromatograms of the unfractionated (part A) and fractionated (part B) inverse starblock copolymers are shown in Figure 3.

The synthesis of the series of linear tetrablocks proceeded in a similar fashion. A dilute solution of PI−PS$^-$Li$^+$ in benzene was added into a large excess of dimethyldichlorosilane, Si(CH$_3$)$_2$Cl$_2$, forming the monofunctional linking agent (PI−PS)Si(CH$_3$)$_2$Cl. Upon examination of this product with SEC, the (PI−PS)Si(CH$_3$)$_2$Cl chromatogram was indistinguishable from the that of the PI−PS$^-$Li$^+$ precursor, indicating no dimer formation. The excess Si(CH$_3$)$_2$Cl$_2$ and benzene were removed on the vacuum line. Then the (PI−PS)Si(CH$_3$)$_2$Cl/benzene solution was reacted with an excess of PS−PI$^-$Li$^+$ to produce the linear tetrablock copolymers. The excess of the PS−PI$^-$Li$^+$ diblock precursor after termination with methanol was removed by fractionation.

The use of chlorosilane for connecting the two diblock arms was preferred over the sequential addition of styrene and isoprene monomers, which could lead to the same tetrablock copolymer but with broader molecular weight distribution and different microstructure of the two PI blocks.[35] It is known that the rate of initiation of the styrene polymerization from the isoprenyllithium is not sufficiently fast when compared to the rate of propagation, to give a narrow molecular weight distribution. A possible way to overcome this difficulty would be by the addition of a small amount of THF prior to the styrene block copolymerization. However, this would affect the microstructure of the next polyisoprene block, giving rise to increased vinyl content. The method described above has the additional advantage that the same diblock precursors used for the inverse starblock copolymer synthesis were also used for the synthesis of the tetrablocks. This ensures that the corresponding tetrablocks and inverse starblocks have the same block components, and therefore, they are directly comparable. The molecular characteristics of the diblock precursors (PS−PI) and (PI−PS) are given in Table 1.

The nomenclature describing our miktoarm block copolymer systems is as follows. The general architecture synthesized is (PS$_{\alpha M}$−PI$_M$)$_n$−(PS$_M$−PI$_{\alpha M}$)$_n$. Linear tetrablocks ($n$ = 1) and inverse starblocks ($n$ = 2) are denoted "TB-α" and "SB-α", respectively. α (=1, 2, 4) is the arm asymmetry parameter. The molecular weight of the inner blocks is approximately 20 000 in all cases. For example, "SB-4" is the miktoarm inverse starblock (PS(80 000)−PI(20 000))$_2$−(PS(20 000)−PI(80 000))$_2$. Exact molecular weights, compositions, and polydispersities of the series of miktoarm block copolymers are shown in Table 2.

TEM micrographs of TB-1/SB-1, TB-2/SB-2, and TB-4/SB-4 are shown in Figure 4. The TEM images demonstrate that the structure of the first five members of the series are lamellar (Figure 4a−e). Each structure is characterized with a single lattice constant ($d$ spacing) and single PS and single PI domain thickness; i.e., there are no multiple sub-repeat spacings. Examination of

**Table 1. Molecular Characteristics of the Diblock Precursors**

| sample | (PS−PI)-4 | (PS−PI)-2 | (PS−PI)-1 |
|---|---|---|---|
| $M_n$(PS) × $10^3$ [a] | 82.0 | 36.1 | 19.4 |
| $M_w/M_n$(PS)(SEC)[c] | 1.03 | 1.03 | 1.04 |
| $M_n$(PS−PI) × $10^3$ [a] | 101 | 52.6 | 38.5 |
| $M_w$(PS−PI) × $10^3$ [b] | 104 | 54.5 | 39.6 |
| $M_w/M_n$(PS−PI)(SEC)[c] | 1.04 | 1.04 | 1.03 |
| wt % PS | | | |
| UV-SEC[c] | 80 | 65 | 48 |
| $^1$H NMR | 80 | 68 | 51 |
| sample | (PS−PI)-4 | (PS−PI)-2 | (PS−PI)-1 |
| $M_n$(PI) × $10^3$ [a] | 73.0 | 32.5 | 18.8 |
| $M_w/M_n$(PI)(SEC)[c] | 1.03 | 1.04 | 1.03 |
| $M_n$(PI−PS) × $10^3$ [a] | 93.1 | 50.0 | 39.3 |
| $M_w$(PI−PS) × $10^3$ [b] | 96.4 | 52.2 | 40.1 |
| $M_w/M_n$(PI−PS)(SEC)[c] | 1.03 | 1.04 | 1.03 |
| wt % PS | | | |
| UV-SEC[c] | 20 | 35 | 51 |
| $^1$H NMR | 21 | 37 | 52 |

[a] Membrane osmometry in toluene at 34 °C. [b] LALLS in THF at 25 °C. [c] SEC in THF at 30 °C.

**Table 2. Molecular Characteristics of the Miktoarm Starblock (SB) and Linear Tetrablock (TB) Copolymers**

| sample | SB-4 | SB-2 | SB-1 |
|---|---|---|---|
| $M_n$ × $10^3$ [a] | 378 | 212 | 148 |
| $M_w$ × $10^3$ [b] | 395 | 220 | 152 |
| $M_w/M_n$ (SEC)[c] | 1.05 | 1.04 | 1.03 |
| wt % PS ($w$) | | | |
| UV-SEC[c] | 48 | 50 | 49 |
| $^1$H NMR | 50 | 49 | 49 |
| $(dn/dc)_c$[d] | 53 | 51 | 51 |
| calcd[e] | 50 | 51 | 50 |
| asymmetry parameter[f] | 4 | 2 | 1 |
| sample | SB-4 | SB-2 | SB-1 |
| $M_n$ × $10^3$ [a] | 201 | 103 | 80.2 |
| $M_w$ × $10^3$ [b] | 213 | 106 | 82.9 |
| $M_w/M_n$ (SEC)[c] | 1.04 | 1.03 | 1.04 |
| wt % PS ($w$) | | | |
| UV-SEC[c] | 51 | 51 | 51 |
| $^1$H NMR | 53 | 52 | 50 |
| $(dn/dc)_c$[d] | 52 | 52 | 53 |
| calcd[e] | 50 | 51 | 51 |
| asymmetry parameter[f] | 4 | 2 | 1 |

[a] Membrane osmometry in toluene at 34 °C. [b] LALLS in THF at 25 °C. [c] SEC in THF at 30 °C. [d] Calculated from: $(dn/dc)_c = w(dn/dc)_{PS} + (1 - w)(dn/dc)_{PI}$ with the values of the refractive index increment, $dn/dc$, and weight fraction, $w$, of the PS and the PI determined in THF at 25 °C. [e] Calculated from the molecular weight of the diblock precursors (Table 1). [f] $\alpha = M_o/M_i$.

many such TEM micrographs shows that, in all cases, the microstructure formed by the starblock copolymer exhibits a grain size smaller than that of the corresponding linear copolymer. This is due largely to the slower kinetics inherent in systems composed of branched copolymers and the fact that each star copolymer is twice the total molecular weight of the corresponding linear copolymer. In such systems, molecular self-assembly is hindered due to the low diffusivity of the branched block copolymers.[36]

The small angle X-ray data show scattering characteristic of a single lamellar repeat spacing for all three TB copolymers as well as the two lower molecular weight starblock copolymers (SB-1 and SB-2). A typical SAXS pattern of this type is shown in Figure 5b. The (00l) Bragg peaks have $q$ values in the ratio of 1:3:5. These ratios are expected for symmetric A/B lamellae since even orders of diffraction are extinguished at 50/50 composition due to form factor cancellation of the even order lattice peaks. The observed SAXS patterns

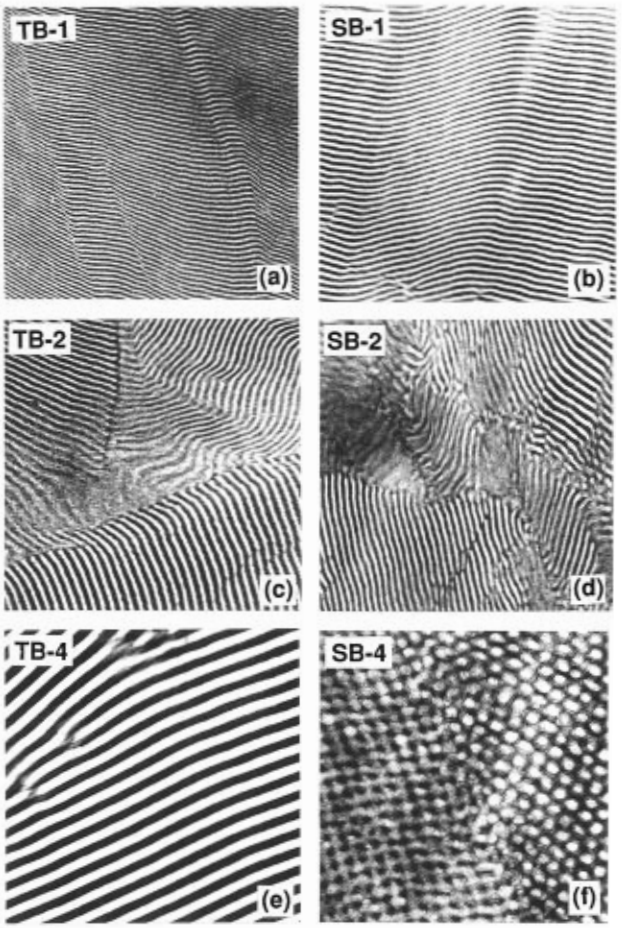


**Figure 4.** (Parts a−f) Bright-field TEM micrographs of the linear tetrablock/miktoarm starblock copolymer pairs. The dark and light regions correspond to the $OsO_4$ stained PI and the unstained PS components, respectively. (f) A region of SB-4 containing adjacent grains exhibiting 4-fold (left) and 3-fold symmetry (right).

indicate a single lamellar long period consistent with the bright-field TEM micrographs.

The values of the (001) $d$ spacings are listed in Table 3. Comparison between the corresponding linear and star copolymers indicates that, for every pair, a significantly smaller $d_{001}$ spacing occurs for the miktoarm star copolymer. Moreover, if we compare the data to lamellar repeat spacings for simple diblock (DB) copolymers of the same approximate overall weight, we find $d_{SB} < d_{TB} < d_{DB}$ (see Table 3 bottom).

The average area of interface per copolymer chain is a measure of the average lateral separation of the copolymer junctions and reflects the nature of the packing environment and the conformation of the A and B blocks of the average chain. The average area per copolymer is the area of the PS-PI interface divided by the number of copolymer molecules on the PS-PI interface. The IMDS area per chain for a lamellar structure of repeat spacing $d_{001}$ is given by:

$$\sigma_i = \frac{2M_{PI}}{d_{001}(1 - \phi_{PS})\rho_{PI}N_A}$$

where $M_{PI}$ is the total molecular weight of all the PI blocks and $N_A$ is Avogadro's number. The average area per junction can be approximated by dividing $\sigma_i$ by the number of junctions per molecule (3 for tetrablocks, 5 for miktoarm stars). The data in Table 3 indicate an

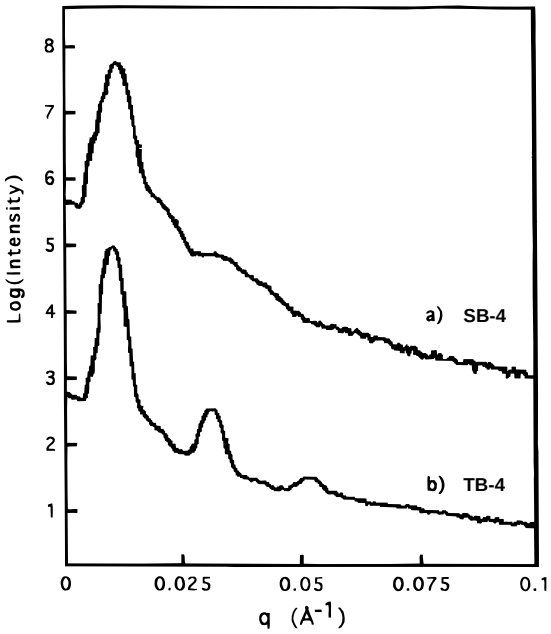


**Figure 5.** SAXS intensity profiles for the TB-4 and SB-4 samples. All frames were radially integrated about the beam center in bins of 1 pixel width. The TB-4 profile exhibits 3 well-resolved peaks consistent with lamellar ordering at 50/50 volume fraction (extinction of even orders of diffraction). The diffraction signature of SB-4 indicates a nonlamellar morphology (see text).

**Table 3. Morphological Characteristics of Tetrablock and Miktoarm Starblock Copolymers**

| sample | $(\chi N)_{\text{calc ODT}}$[a] | $\chi N$ (120 °C)[b] | $d_{001}$ (Å) | $\sigma$/chain (Å$^2$) | $\sigma_{\text{average}}$/junction (Å$^2$) |
|---|---|---|---|---|---|
| TB-1 | 25 | 74 | 235 | 1235 | 412 |
| SB-1 | 26 | 144 | 222 | 2615 | 523 |
| TB-2 | 19 | 88 | 322 | 1091 | 397 |
| SB-2 | 19.5 | 182 | 305 | 2515 | 503 |
| TB-4 | 13 | 153 | 635 | 1230 | 410 |
| SB-4 | 13.5 | 326 | 545[c] | 3100[c] | 620[c] |
| PS/PB,[d] 42.3/45.4 | 10.5 | 60 | 625 | 501 | 501 |
| PS/PB[d] 20.5/20.5 | 10.5 | 28 | 387 | 378 | 378 |

[a] See ref 32. [b] $\chi_{SI}$(120 °C) ≃ 0.074 (from ref 41). [c] Cubic microdomain structure. [d] $\chi_{SB}$ (120 °C) ≃ 0.047 (from ref 42).

increase of area per junction with molecular weight and with star compared to linear tetrablock architecture and with linear tetrablock compared to simple diblock architecture.

This trend in *d* spacing can be understood in terms of the relative number of bridge vs loop conformations for the interior blocks of the SB and TB copolymers in a lamellar structure.[37] As α increases, the ability of the shorter interior blocks to bridge the domain decreases, so more loop conformations occur. The consequence of looped interior blocks is that all of the peripheral junctions are located on the central junction interface. These loop conformations force the A/B junctions further apart on average, and therefore the long exterior blocks can assume less stretched conformations. For SB-α copolymers, the juxtaposition of 4 peripheral junctions about the central junction likely causes the peripheral junctions to move even further apart to avoid overcrowding in comparison to the corresponding TB-α copolymers, which only have 2 peripheral junctions (see schematic drawing, Figure 6). The larger number of peripheral junctions decreases the lamellar repeat distance, and this increases the area of IMDS per chain of SB-α over TB-α (Table 3).

The scattering pattern for SB-4 is significantly different than that for a lamellar structure. The SAXS intensity profile shows a strong, broad low angle diffraction peak, suggestive of several superposed peaks followed by a shoulder and a weaker asymmetrically broadened peak at high scattering angle, *q*. The *d* spacing of the first peak occurs at approximately 545 Å, considerably smaller than the 635 Å (001) spacing of the corresponding tetrablock TB-4. This diffraction signature indicates that the morphology of SB-4 is nonlamellar. Unfortunately, the number of resolved reflections in the SAXS pattern is inadequate to determine a structural assignment.

TEM micrographs of SB-4 show a complicated domain structure with a highly curved IMDS. TEM is a local technique for structural investigation and has the advantage that one can select regions of better order for detailed analysis. For example, TEM micrographs of SB-4, such as Figure 4f, frequently exhibit 4-fold and 3-fold symmetric projections—a characteristic signature of a microphase with cubic symmetry. The image contrast of figure 4f suggests continuous polyisoprene and discrete polystyrene microphases, but other regions show the lighter PS phase to be continuous.

The structural symmetry of SB-4 was also investigated through optical birefringence measurements. The largest contributor to the total birefringence in a block copolymer is normally the form birefringence. If the microdomains adopt a cubic structure, then because all second rank tensor properties of cubic crystals are isotropic, the form birefringence will be zero. To within the precision of the birefringence measurements, films of SB-4 exhibited no birefringence, indicating that the material is either homogeneous or cubic since it is optically isotropic. In contrast, measurements performed on the other inverse starblock and tetrablock copolymer samples exhibited optical anisotropy (nonzero birefringence) as expected for systems forming lamellar microdomains.

The PS phase continuity of sample SB-4 was also investigated by modulus measurements. For a discrete PS microdomain structure, e.g., PS spheres on a cubic lattice, the sample modulus is dictated by that of the rubbery matrix material. For a three-dimensionally continuous PS microdomain structure, e.g., a PS tricontinuous cubic, the modulus of the copolymer would be dominated by the rigid glassy phase. The experimental values of the modulus are quite consistent with the three-dimensionally continuous PS geometry. A full accounting of the detailed structure of sample SB-4 as determined by comparison of projections of the various candidate cubic model structures as a function of projection direction, section thickness, and location of the section within the unit cell with TEM micrographs will be given elsewhere.[38]

The area per chain in the tricontinuous cubic structure can be estimated assuming that the structure is one of the two known tricontinuous cubics occurring in A/B diblock copolymers with an A/B IMDS of constant mean curvature cmc. Anderson et al.[39] and Groβe-Brauckmann[40] investigated the relationship between mean curvature, interfacial area, and volume fraction for constant mean curvature surface families of the D and G minimal surfaces, respectively. They computed the dimensionless mean curvature $H^*$ and surface area $S^*$ per unit cell, from which the actual mean curvature $H$ and surface area $S$ are given by:

$$H = H^*/2a \qquad S = a^2 S^*$$

where $a$ is the appropriate cubic lattice parameter. The

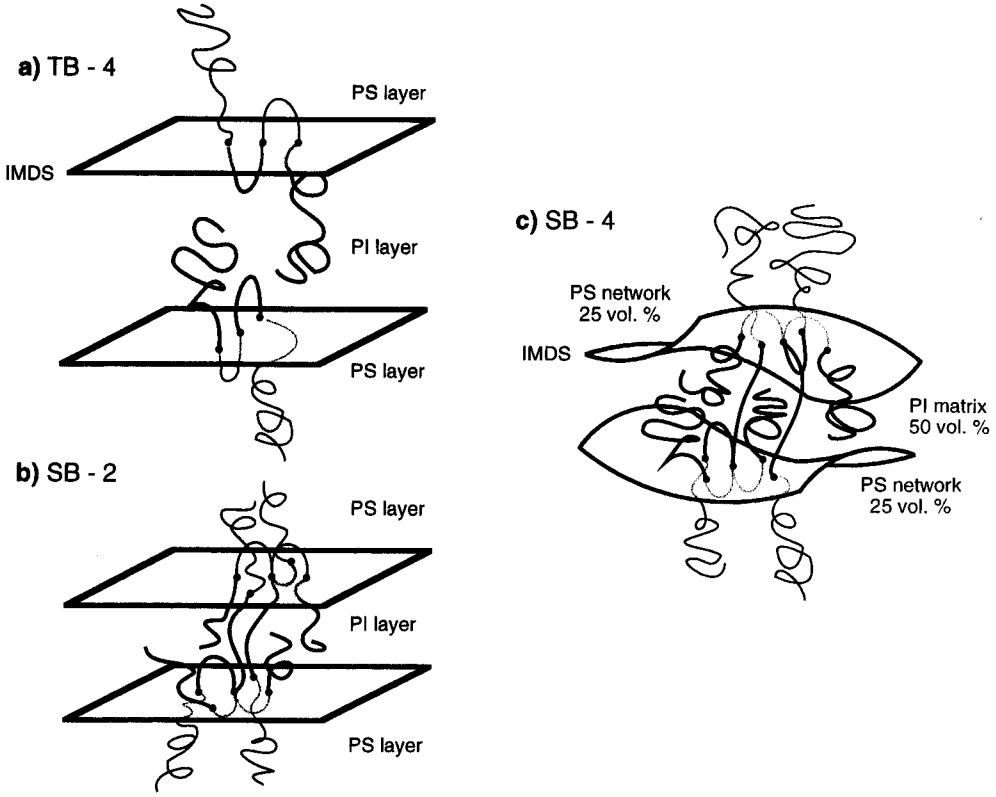


**Figure 6.** Schematic of proposed arrangement of A/B junctions on a flat IMDS for the (a) TB-4 lamellar (all interior blocks form loops) and (b) SB-2 lamellar structures (interior blocks form bridges and loops). (c) Portion of a triply periodic IMDS of constant mean curvature for the SB-4 structure (interior blocks form bridges and loops).

dimensionless surface area $S^*$ is the surface area per volume to the 2/3 power. This quantity is independent of scale of the structure but does depend on the particular choice of fundamental cell. A convenient choice for both the lamellar and cubic geometries is a translational fundamental cell of unit volume. For an A/B lamellar structure the translational fundamental cell is the unit cube which yields a $S/V^{2/3}$ of 2.0. The fundamental translational cell of the D family is a rectangular box comprised of 2 cubes, and the cell of the G family is a rectangular box comprised of 4 cubes. For this choice of normalization, Gro$\beta$e-Brauckmann finds $S/V^{2/3}$ values of 2.42 and 2.45 for the D and G minimal surfaces, respectively. For a tricontinuous morphology with volume fractions of 0.25/0.50/0.25, Gro$\beta$e-Brauckmann's results for the familes of cmc surfaces can be used to compute $S^*$ as 3.35 for the DD and $S^*$ as 5.47 for the DG structure.

The interfacial area per chain for cubic structures is given by:

$$\sigma_i = \frac{S^* M_{PI}}{a(1-\phi_{PS})\rho_{PI} N_A}$$

where $a$ is the appropriate lattice parameter ($a = 2^{1/2} \times 545$ Å for DD and $a = 6^{1/2} \times 545$ Å for DG). Both the DD and DG cmc cubic structures have an average interfacial area per chain for the SB-4 sample of approximately 3100 Å$^2$. We can estimate the interfacial area per chain for a SB-4 sample with a hypothetical lamellar structure by extrapolating the lamellar $d_{001}$ spacing on the basis of the SB-1 and SB-2 samples. This gives an estimate of 471 Å for the hypothetical lamellar repeat of SB-4. The corresponding interfacial area per chain is then 3120 Å$^2$, nearly *the same* as found for the tricontinuous cubic interfacial area. For the other TB/SB pairs of smaller arm asymmetry which maintain a lamellar structure, the average area per junction for the flat lamellar IMDS increases by a factor of about 1.3 as the architecture changes from linear to star. The estimated *area per junction* of the curved IMDS of SB-4 is about 1.5 times higher than for the flat TB-4 IMDS structure.

Thus five of the 50/50 symetric composition copolymers exhibit the normal, flat IMDS lamellar structure, while the sixth copolymer exhibits a novel tricontinuous structure featuring a curved IMDS. The *key architectural feature* driving the transformation from the lamellar to the tricontinuous cubic structure is proposed to be the *large arm asymmetry of the star copolymer.* In Figure 6a,b, the tetrablock copolymer TB-4 ($n = 1$, $\alpha = 4$), and the starblock SB-2 copolymer ($n = 2$, $\alpha = 2$), are shown with their two or four difunctional peripheral A/B junctions on a flat IMDS which minimizes the interfacial energy contribution to the total free energy. The schematics depict the interior blocks of the more asymmetric arm TB-4 molecule in loop conformations, while the less asymmetric arm SB-2 molecule has both loop and bridge interior block conformations.

The lamellar structure is disfavored at $\alpha = 4$ for the star block because the 4 short interior blocks would be too overcrowded as loops on a flat IMDS and/or would be too stretched to form bridges across the thick lamellar domain at this high outer block molecular weight. In order to avoid such overcrowding and stretching, we suggest two things happen: the IMDS becomes curved, allowing the peripheral junctions to spread further apart than on a flat interface, and the microdomain structure becomes triply periodic, which allows more spatial orientations of the chain trajectories and provides opportunities for some bridging of the interior blocks which also serves to relieve overcrowding.

The preferred IMDS structure for sample SB-4 is depicted in Figure 6c. The interfaces shown represent patches of the IMDS having nearly constant mean

curvature, satisfying the requirement that the structure have the lowest possible interfacial area at a particular volume fraction and symmetry.[26] The miktoarm star-block may arrange its five junctions on several nearby interfaces of the interpenetrating labyrinthine networks of the tricontinuous cubic structure using both loop and bridge conformations for the interior block. This choice of curved interface structure yields an interfacial area comparable to the estimated flat IMDS for a lamellar structure for this architecture and arm asymmetry while the reduction in the entropic contribution of the interior blocks to the free energy drives the transition.

## Conclusions

A series of six well-defined, compositionally symmetric polystyrene−polyisoprene block copolymers having both linear and star architectures was synthesized using anionic polymerization and cholorosilane chemistry in order to induce a new strongly segregated, *nonlamellar* microdomain structure at 50/50 volume fraction. Five of the copolymers were found to exhibit a lamellar microdomain morphology. The sixth, a miktoarm inverse star with the highest molecular weight asymmetry between the outer and inner blocks of the arms, exhibited a nonlamellar morphology.

X-ray scattering of the nonlamellar inverse starblock was inconclusive as to a structural assignment due to insufficient peak resolution. TEM images which exhibited both 3- and 4-fold rotational symmetry, along with optical measurements of zero birefringence of the structure and modulus measurements indicating a continuous PS microdomain geometry, suggested a tricontinuous cubic structure.

The transformation from the flat IMDS structure of a lamellar phase to the curved IMDS structure of a tricontinuous cubic microdomain morphology was proposed to result from the need to avoid overcrowding of looped-interior blocks and/or to avoid the extreme stretching of bridged-interior blocks in the star block copolymer at the highest degree of arm asymmetry and outer arm molecular weight. A tricontinuous microdomain structure lowers the entropic contribution of the interior blocks to the overall free energy because the peripheral junctions can move further apart on a curved IMDS and because the distances and directions between nearby regions of the IMDS are close enough and numerous so that the interior blocks can form some bridges.

**Acknowledgment.** The authors would like to thank M. Capel (BNL) and B. L. Carvalho (MIT) for assisting in the X-ray characterization. We also thank L. Radzilowski and C. Lambert for help with level surfaces and J. Chen for performing the birefringence and optical transforms. Financial support was received from the Greek General Secretariat of Research and Technology, the Research Committee of the University of Athens, NSF DMR (92-14853), AFOSR F49620-94-1-0224, and F49620-94-1-0357, and the Alexander von Humboldt-Stiftung. Work at BNL was supported by a grant from the DOE.

## References and Notes

(1) Leibler, L. *Macromolecules* **1980**, *13*, 1602.
(2) Fredrickson, G. H.; Helfand, E. *J. Chem. Phys.* **1987**, *87*, 697.
(3) Bates, F. S.; Fredrickson, G. H. *Annu. Rev. Phys. Chem.* **1990**, *41*, 525.
(4) Thomas, E. L.; Lescanec, R. L. *Philos. Trans. R. Soc. London A* **1994**, *348*, 149.
(5) Binder, K. *Adv. Polym. Sci.* **1993**, *112*, 181.
(6) Thomas, E. L.; Alward, D. B.; Kinning, D. J.; Martin, D. C.; Handlin, D. L.; Fetters, L. J. *Macromolecules* **1986**, *19*, 2197.
(7) Alward, D. B.; Kinning, D. J.; Thomas, E. L.; Fetters, L. J. *Macromolecules* **1986**, *19*, 215.
(8) Kinning, D. J.; Thomas, E. L.; Alward, D. B.; Fetters, L. J.; Handlin, D. L. *Macromolecules* **1986**, *19*, 1288.
(9) Herman, D. S.; Kinning, D. J.; Thomas, E. L.; Fetters, L. J. *Macromolecules* **1987**, *20*, 2940.
(10) Anderson, D. M.; Thomas, E. L. *Macromolecules* **1988**, *21*, 3221.
(11) Hajduk, D. A; Harper, P. E.; Gruner, S. M.; Honeker, C. C.; Thomas, E. L.; Fetters, L. J. *Macromolecules* **1995**, *28*, 2570.
(12) Matsushita, Y.; Takasu, T.; Yagi, K.; Tomioka, K.; Noda, I. *Polymer* **1994**, *35*, 2862.
(13) de la Cruz, M. O.; Sanchez, I. C. *Macromolecules* **1986**, *19*, 2501.
(14) Milner, T. S. *Macromolecules* **1994**, *27*, 2333.
(15) latrou, H.; Hadjichristidis, N. *Macromolecules* **1992**, *25*, 4649.
(16) latrou, H.; Hadjichristidis, N. *Macromolecules* **1993**, *25*, 2479.
(17) Tselikas, Y.; Hadjichristidis, N. *J. Chem. Phys.*, in press.
(18) Yin, R.; Hogen-Esch, T. E. *Macromolecules* **1993**, *26*, 6952.
(19) Hadjichristidis, N.; Iatrou, H.; Behal, S. K.; Chludzinski, J. J.; Disko, M. M.; Garner, R. T.; Liang, K. S.; Lohse, D. J.; Milner, S. T. *Macromolecules* **1993**, *26*, 5812.
(20) Hasegawa, H.; Tanaka, H.; Yamasaki, K.; Hashimoto, T. *Macromolecules* **1987**, *20*, 1651.
(21) Spontak, R. J.; Smith, S. D.; Ashraf, A. *Macromolecules* **1993**, *26*, 956.
(22) Matsushita, Y.; Tamura, M.; Noda, I. *Macromolecules* **1994**, *27*, 3680.
(23) Shultz, M. F.; Bates, F. S.; Almdal, K.; Mortensen, K. *Phys. Rev. Lett.* **1994**, *73*, 86.
(24) Förster, S.; Khandpur, A. K.; Zhao, J.; Bates, F. S.; Hamley, I. W.; Ryan, A. J.; Bras, W. *Macromolecules* **1994**, *27*, 6922.
(25) Winey, K. I.; Thomas, E. L.; Fetters, L. J. *Macromolecules* **1992**, *25*, 422.
(26) Thomas, E. L.; Anderson, D. M.; Henkee, C. J.; Hoffman, D. *Nature* **1988**, *334*, 598.
(27) Hajduk, D. A.; Harper, P. E.; Gruner, S. M.; Honeker, C. C.; Kim, G.; Thomas, E.L.; Fetters, L. J. *Macromolecules* **1994**, *27*, 4063.
(28) The G minimal surface has space group $I4_132$ considering the surface as orientable. The space groups $I4_132$ and $Ia\bar{3}d$ differ only by the presence of an inversion center in $Ia\bar{3}d$.
(29) Longley, W.; McIntosh, T. J. *Nature* **1983**, *303*, 612.
(30) Charvolin, J.; Sadoc, J. F. *J. Phys.* **1987**, *48*, 1559.
(31) Seddon, J. M. *Biochim. Biophys. Acta* **1990**, *1031*, 1.
(32) Calculated using mean-field density functional theory (DFT) with the vertex function $\Gamma_2$ appropriate to the miktoarm starblock/linear tetrablock architecture considered. For further discussions of DFT of microphase separation in block copolymers, see: Melenkevitz, J.; Muthukumar, M. *Macromolecules* **1991**, *24*, 4199.
(33) Capel, M. S.; Smith, G. C.; Yu, B. *Rev. Sci. Instrum.* **1995**, *66*, 2295.
(34) Roovers, J. E. L.; Bywater, S. *Macromolecules* **1972**, *5*, 384.
(35) Spontak, R. J.; Smith, S. D.; Satkowski, M. M.; Ashraf, A.; Zielinski, J. M., *Polymer Solutions, Blends and Interfaces*; Noda, T., Rubingh, D. N., Eds.; Elsevier: Amsterdam, 1992; p 65.
(36) Factor, B. J.; Russell, T. P.; Smith, B. A.; Fetters, L. J.; Bauer, B. J.; Han, C. C. *Macromolecules* **1990**, *23*, 4452.
(37) Matsen, M. W.; Schick, M. *Macromolecules* **1994**, *27*, 187.
(38) Thomas, E. L.; Hadjichristidis, N., et al. In preparation.
(39) Anderson, D. M.; Davis, H. T.; Scriven, L. E.; Nitsche, J. C. C. *Adv. Chem. Phys.* **1990**, *77*, 337.
(40) Groβe-Brauckmann, K. *The Family of Constant Mean Curvature Gyroids*; GANG Preprint; University of Massachusetts: Amherst, 1995.
(41) Mori, K.; Hasegawa, H.; Hashimoto, T. *Polym. J.* **1985**, *17*, 799.
(42) Wolff, T.; Burger, C.; Ruland, W. *Macromolecules* **1993**, *26*, 1707.

MA9515083